Progress In Electromagnetics Research, Vol. 139, 599–610, 2013

PMM-GA METHOD TO SYNTHESIZE QUASI-OPTICAL FREQUENCY SELECTIVE SURFACE ON SiO_2 SUBSTRATE

Bu Gang Xia[1, 2, *], Jin Meng[1, 2], De Hai Zhang[1], and Jin Sheng Zhang[3]

[1]Key Lab. of Microwave Remote Sensing, Center for Space Science and Applied Research, Chinese Academy of Sciences, Beijing, China

[2]University of the Chinese Academy of Sciences, Beijing, China

[3]China Academy of Space Technology, Beijing, China

Abstract—A satellite-borne frequency selective surface (FSS) for atmospheric sensing application is presented. This brand new type of band-pass filter has an operating frequency at 183 GHz, which is a typical frequency on H_2O absorption line. Comprising an ultra-thin gilding layer and a SiO_2 substrate layer, this complex periodic component exhibits an extremely low insertion loss (< 0.22 dB) and high isolation (> 20 dB) between closely spaced frequency channels of 45° incident wave. Periodic Method of Moment (PMM) approach is applied to determine the initial geometrical parameters of FSS unit cell, and the optimization approach based on the Genetic Algorithm (GA) enables us to obtain the requisite spectral response and transmission characteristics for both TE and TM polarization. The experimental results show that the proposed PMM-GA technique is effective for analyzing space-borne FSS at millimeter wave range.

1. INTRODUCTION

As acting a spatial microwave and optical filter, Frequency selective surface (FSS) has been intensively investigated over the past decades [1, 2] for its huge prospect in space science applications. Conducting screen (either freestanding or supported by dielectric layers) periodically perforated with apertures, or an array of metallic patch elements of arbitrary geometries, constructs a FSS filter to

Received 27 March 2013, Accepted 6 May 2013, Scheduled 13 May 2013

* Corresponding author: Bu Gang Xia (xiabugang09@mails.ucas.ac.cn).

electromagnetic (EM) waves. The overall frequency properties (e.g., transmission coefficient, bandwidth, phase feature and angle stability) of the structure depend on many crucial parameters, such as unit cell's pattern, array periodicity, element geometry sizes, as well as properties of dielectric substrate. Therefore, to synthesize FSS with a desired frequency characteristic, one typically resorts to an error procedure and tedious trial, since few systematic alternatives are currently available for this purpose. The conventional FSS design techniques have a common character that they focus on the simplest type of resonance unit cell, for instance, unit cells consisted of resonant loops [3], dipoles of different shapes [4] or fractals, and Jerusalem crosses [5] are among the most extensively used pattern type building units of FSS designed utilizing traditional techniques.

In general, the size of the resonant unit cells and the inter-cell spacing are comparable to one-third of half a wavelength in such structures at the expected operation frequencies. However, because of the multitudinous parameters, these commonly employed matrixes can hardly meet the desired requirements in practical applications. The objective of this paper is to describe a novel approach, which is based on the combination of genetic algorithm (GA) [6] and Periodic Method of Moment (PMM), for synthesizing space-borne FSS filter on SiO_2 substrate.

GA is a robust stochastic, iterative and evolutional process imitated on the principles of natural selection and population genetics mechanism. As an optimizer, GA is useful for solving complicated combinational problems where numerous parameters must be optimized simultaneously, and problems which can not possess a unique, well-defined optimum. It is especially efficient in searching for maxima in 3D finite element model domains. GA has been used to solving optimization problems in electromagnetic [7] for a period of time. In particular, GA techniques have been proven extremely useful for designing FSS with optimal propagation properties. The PMM-GA-based FSS optimization approach offers several advantages over the existing design methods. GA usually has the strict theoretical basis, not just with expert experience (such as the proposed conventional techniques), and in theory can finally find the optimal solution or approximate optimal solution.

GA approach with an improved Fitness Function (FF_{GA}) to optimize the initial FSS designed by PMM is proposed in this paper. As a numerical method, PMM can be applied in conjunction with GA to provide a powerful tool for the design optimization of dielectric-based FSS for remote sensing applications. A new type of millimetre wave space-borne FSS with low loss and higher transmission frequency

response is presented. The frequency feature of this periodic structure is less sensitive to the angle of incidence of the EM wave compared to other band-pass FSS filter designed using conventional design techniques. The flowchart of FSS design process utilizing GA approach is shown in Figure 1, and it would be detailed described in next section.

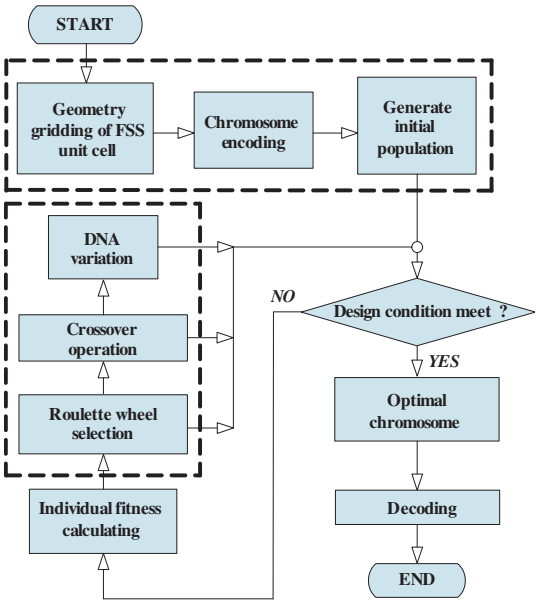

Figure 1. The flowchart of FSS optimization cycle using Genetic Algorithm approach.

2. FORMULATIONS AND METHODOLOGIES

The applications of the before-mentioned design methodologies are illustrated for achieving a novel FSS filter in this part. Unlike the component which consists of freestanding metallic arrays, this class of FSS is dielectric-loaded with PMM-GA-based periodic unit cells. Because this kind of FSS can lightly be designed to operate at large angles of incidence at band pass mode. Meanwhile, to satisfy the current required performance specifications, the FSS should present minimum insertion loss at $F_{pass} = 183\,\text{GHz}$, and control stop band damping larger than 15 dB at $F_{stop} = 230\,\text{GHz}$. The geometry size of the unit cell is depicted in Figure 3(a).

The ultimate evolutionary individual of FSS unit cell contains two conterminous layers (see Figure 2): a 3 µm gilding layer, perforated

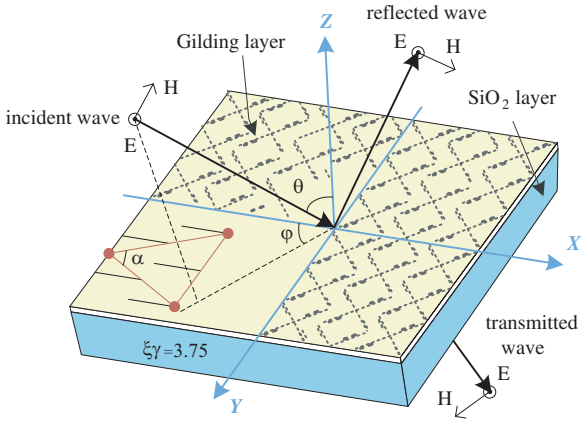

Figure 2. Schematic diagram of FSS radiated by oblique incident wave.

with PMM-GA based pattern. The gilding layer is overlayed on an electrically thick SiO_2 wafer layer [8], with relative dielectric permittivity $\varepsilon_r = 3.75$. Since it is rigid, properly low dielectric loss (loss tangent $\tan\delta = 20\times10^{-4}$) and high resistivity, SiO_2 is a desirable dielectric material as backing substrate for space science components. Moreover, it also can be furbished to furnish an optically glossy surface.

Now the formulation of scattering to FSS screen at millimetre waves (MMW) range should be considered in detail. To calculate the frequency characteristics of FSS screen, numerical method is followed by the well established procedure of solving the Electric Field Integral Equation (EFIE) [9] derived by enforcing Floquet's [10] periodicity condition in an elementary unit cell. As shown in Figure 2, it is supposed that FSS screen lying in the x-y plane with array periodicities L_x and L_y along the x and y directions, respectively. The EFIE for the current distributions on perfectly conducting surface can be figure up in the form followed:

$$-\begin{bmatrix} E_x^i(x,y) \\ E_y^i(x,y) \end{bmatrix} = \frac{2\pi}{j\omega\varepsilon_0 L_x L_y}\sum_m\sum_n \begin{bmatrix} k_0^2-\alpha_m^2 & -\alpha_m\beta_n \\ -\alpha_m\beta_n & k_0^2-\beta_n^2 \end{bmatrix} \times G(\alpha_m,\beta_n)\begin{bmatrix} J_x(\alpha_m,\beta_n) \\ J_y(\alpha_m,\beta_n) \end{bmatrix}\cdot e^{j\alpha_m x}\cdot e^{j\beta_n y} \quad (1)$$

$$\alpha_m = \frac{2\pi m}{L_x} + k_0\sin\theta\cos\varphi \quad (2)$$

$$\beta_n = \frac{2\pi n}{L_y} + k_0 \sin\theta \cos\varphi \tag{3}$$

where $E_x^i(x,y)$ and $E_y^i(x,y)$ denote the x and y components, respectively, of the electric field radiates on the FSS screen, while θ and φ are the angles of the incident EM wave (shown in Figure 2). Moreover, $G(\alpha_m,\ \beta_n)$ is the dyadic spectral Green's function that accounts for the presence of the lossy dielectric substrate upon which the FSS arrays are plated. Equation (1) must be solved for the distributions of current J_x and J_y after positioning suitable master and slave boundary conditions on the surface of FSS's profiles. Particularly, current distributions of J_x and J_y can be expressed by:

$$J_x = \sum_m \eta_m \exp\left[j\left(\frac{2m\pi}{L_x} + k_x\right)x\right] \tag{4}$$

$$J_y = \sum_n \eta_n \exp\left[j\left(\frac{2n\pi}{L_y} + k_y\right)y\right] \tag{5}$$

where η_m and η_n are coefficients of the Fourier series, and k_x and k_y represent the propagation constants of Floquet mode. A GA-based optimization flowchart is demonstrated for the synthesis of the required resonant structures. Above all, the structural dimensions and geometry parameters of unit cell must be numerically calculated, according to [11], array periodicities L_x and L_y ($L_x = L_y$) can be estimated by:

$$L_x = \frac{c}{F_{stop}\left(\sqrt{\varepsilon_r} + \sin\theta\sin\varphi\right)} \tag{6}$$

where c is the speed of the light (3×10^8 m/s). For TE polarization at 45° incidence (i.e., $\theta = 45°$) and under the condition $\varphi = 0°$, the required size of unit cell turn out to $L = 674\,\mu$m. Then, the next step is to divide a single FSS unit cell into linked pixels (all the same size), also called grid subdivision. This is an extra crucial step to establishing proper population size. Not only to reduce the total convergence time of optimization processes, paradoxically, but also to ensure the accuracy of the optimized result, the grid subdivision should be down correctly. In practical, as showing in Figures 3(a) and (c), the $L \times L$ region is divided into 20×20 grid of square pixels preparing for chromosome encoding. Figures 3(d) and (f) can explain the correspondence between the decoded FSS unit cell and the chromosome.

To obtain polarization independent performance, the GA approach operates on 1/4 region of the unit cell geometry, i.e., 10×10 grids. So the GA-operated 1/4 unit cell is encoded into a binary string

with 100 bits, namely, 100 DNAs. And the remaining three regions of the unit cell are constituted by rotating the GA-operated region by 90°, 180° and 270°, respectively. The 10×10 GA-operated 1/4 region is encoded in terms of 1 s and 0 s. The 1 and 0 correspond to the metallic conducting surface (blue pixels in Figure 3) and the free space (other pixels except blue pixels), respectively. Generally, evaluation of the FSS unit is accomplished via FF_{GA}, which is defined as the minimum value of reflection or maximum transmission coefficient in each specified band. The FF_{GA} [12] used in GA for synthesizing high transmissibility band-pass FSS can given by:

$$FF_{GA} = \min\left(\sum_{\substack{\text{attenuation band} \\ TC>0.16}} (TC-0.16)^{\frac{1}{2}} + \sum_{\substack{\text{transmission band} \\ TC<0.93}} (0.93-TC)^{\frac{1}{2}} \right) \tag{7}$$

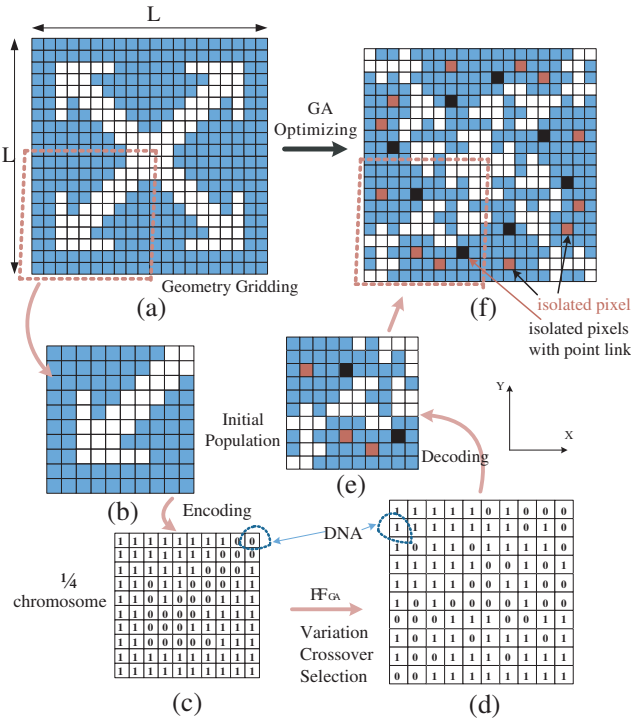

Figure 3. FSS synthesize process. (a) Initial population generated by PMM. (b) 1/4 region of the unit cell. (c) Encoding process. (d) Optimized unit cell. (e) Decoding procedure. (f) The ultimate evolutionary unit cell.

It can be seen from Equation (7) that TC is the abbreviation of transmission coefficient. The structures of FSS element with the required characteristics generate through Roulette Wheel Selection (RWS) [13], which is a standard proportionate selection of GA approach. Moreover, to achieve a realistic design, the crossover operation was included in the FSS optimization procedure cycle, with a cross probabilities $P_{cross} = 80\%$ and the mutation rate $P_{mutation} = 2\%$. If the FF_{GA} reaches value that satisfied for the design conditions at each single generation, then the optimized structure of FSS unit cell is acquired. Otherwise, the optimization routine is repeated until the desired chromosome of FSS is achieved. Figure 3(a) shows the original design result of FSS structure. A full-wave PMM-based computer code [14] has been employed in this study to actualize the electromagnetic simulations of the candidate FSS unit cell and generate the original design, i.e., initial population. Accordingly, Figure 3(f) is showing the optimized structure of FSS unit cell created by GA-based optimization process.

3. EPERIMENTAL RESULTS

Some experimental results to demonstrate the efficiency of the proposed optimization procedure are illustrated in this section. The design specifications call for the pass-band FSS to perform accurately in MMW range. Specifically, it is desired that the FSS provides a high transmission coefficient from 171 GHz to 201 GHz.

FSS screen should be placed in a focused beam for real space applications, so it is important to know behavior of FSS for oblique incident angles other than normal case ($\theta = 0^\circ$). Mostly, the incident angle is set as 45°. The solution generated by the GA after 200 generations of evolution process is exhibited (see Figure 3), which shows the shape of the unit describing the basic periodicity cell. Considering not to yield the grating lobe [15, 16] in the desired band, the optimum dimension of the unit cell is fixed at $L = 660\,\mu m$. In addition, the thickness of the SiO_2 substrate is chosen at 368 µm.

It should be noted that the isolated pixels either with point contacts (black pixels) or without point contacts (red pixels) exist as shown in Figures 3(e) and (f). To achieve a more practical design than a scattershot design and to get rid of unnecessary complexity of fabrication, all of these isolated pixels [17] can be removed from unit cell. However, even if the physically-isolated pixels exist in this optimized FSS structure, these pixels can be ignored electrically and physically because their currents cannot be inherently modelled in the simulation. Therefore, GA automatically selects the geometry-refined

unit cell according to the desired specifications. In Figure 4, a partial photography of FSS screen which fabricated without these isolated pixels is shown, and the frequency characteristics of this FSS sample are measured (see Figure 8).

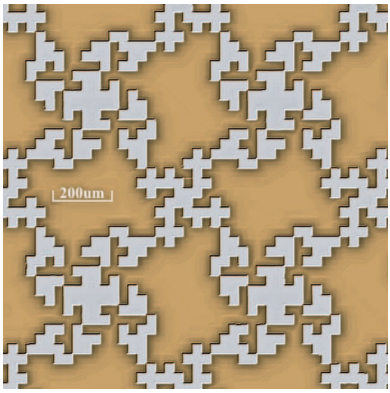

Figure 4. Photography of FSS segment (top view).

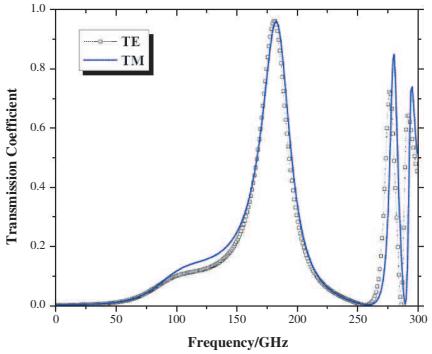

Figure 5. Numerical results of FSS screen in Figure 3 for both TE and TM polarizations at an incidence angle of 45°.

Under specified conditions for both TE and TM polarizations at 45° incidence, the transmission coefficients (numerical results) are plotted in Figure 5, which shows a desired transfer function and polarization independence of the of the PMM-GA-based FSS. For TE wave, the 3 dB bandwidth (BW) is 33 GHz. Meanwhile, the other three characteristic parameters are exhibited specifically in Table 1. IL is the insertion loss of FSS filter, F_{pass} the resonant frequency, and TC the transmission coefficient which has already been discussed in previous section. According to Table 1, it can be seen that resonance occurs at 183.5 GHz for TE excitation ($\theta = 45°$), and the insertion loss is about 0.17 dB, as well as power conversion efficiency $TC = 0.961$. There is a slight alteration in TM case, on which the FSS is provide a 3 dB bandwidth of 32 GHz (approx. from 168 GHz to 200 GHz), insertion loss [18, 19] of 0.21 dB, and operating frequency of 184.3 GHz, which could be acceptable in practical applications. The frequency response curves of S parameters for full wave at 45° incidence are reported in Figure 6. The transmission and reflection spectra contain a desired pass-band at about 183 GHz.

Figure 7 shows the comparison of frequency characteristics

Table 1. Transfer feature comparison of FSS exited by TE and TM polarized wave.

Mode	θ	φ	$\boldsymbol{F}_{pass}$	***IL***	***TC***
TE	45°	0°	183.5 GHz	0.17 dB	0.961
TM	45°	0°	184.3 GHz	0.21 dB	0.953

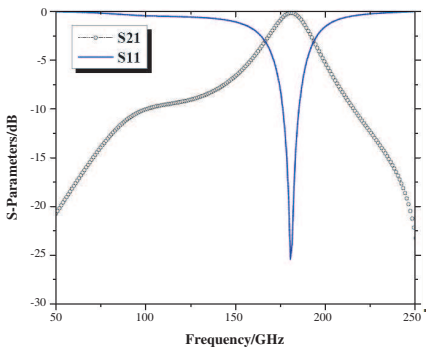

Figure 6. S parameter (S_{21} and S_{11}) given in dB as a function of frequency at 45° incidence.

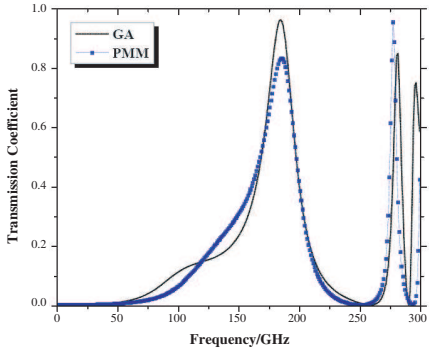

Figure 7. Characteristic of FSS (designed by PMM) is shown together with transmission coefficient (optimized by GA).

between the FSS designed by PMM and GA-based FSS. These two corresponding FSS structures are shown in Figure 3(a) and Figure 3(f), respectively. By GA optimization, the transmission coefficient rise from 0.834 to 0.961, up by 15.23% in proportion, the power conversion efficiency has a significantly improvement, and the amplitude of grating lobe is lowered around 275 GHz.

Figure 8 shows the measured transmission coefficient of the GA-based FSS along with the full-wave EM simulation results procured by PMM code. As is showing in the figure, a considerably good agreement between the numerical values and measured results is observed. The deviations between the numerical and measured results are mainly at the peak of transmission curves. The discrepancy is attributed to the leakage from the apertures that exist between the edges of the metallic slots and the SiO_2 wafer layer, scattering from the edges of the screen, as well as the finite size of this FSS filter.

The transmission characteristics of GA-based FSS are also

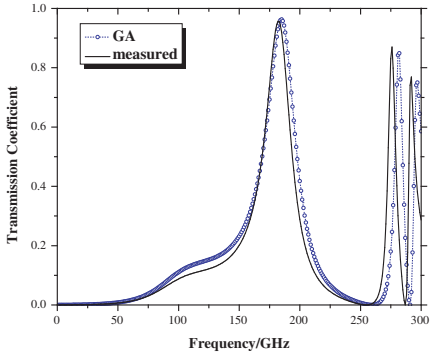

Figure 8. Measured and simulation transmission coefficients of GA-based FSS sample.

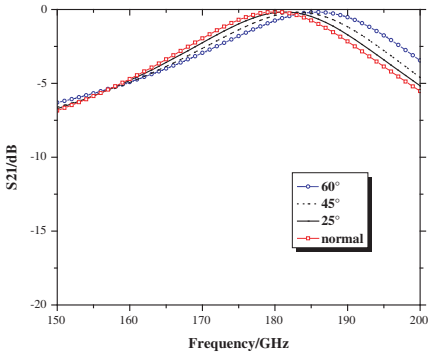

Figure 9. Measured transmission characteristics of GA-based FSS (various angles of incidence at normal/25°/45°/60°, respectively).

measured for various incident angles [20] and the results are presented in Figure 9. As observed from this figure, the frequency response of the FSS is not considerably affected as the angle of incidence increases from 0° to 60°. As θ increasing, the response starts to deviate from that of the normal incidence. Nevertheless, GA-based FSS demonstrates a stable frequency response as a function of angle of incidence.

4. CONCLUSION

A PMM-GA-based quasi-optical FSS filter with adequate band-pass behavior at MMW range is demonstrated in this paper. The analysis of scattering from FSS's surface is solved by electromagnetic solver PMM. For the synthesis of this space-borne FSS, a robust GA optimization process is presented to optimize the topology and dimensions of unit cell, and the optimization process is presented in detail. Using a GA optimization procedure cycle, FSS can be designed to be competent a wide sort of prescribed design indexes, including the F_{pass}, BW, TC, surface impedance, and transmission loss. Compared with traditional FSS filter, this design shows a desired transfer function with less transmission loss and high polarization independence for TE and TM polarized wave at both normal and oblique incidence. This type of PMM-GA-based FSS can be employed in the multichannel quasi-optics network of space-borne radiometers to contribute the performance enhancement required from system.

ACKNOWLEDGMENT

This work is supported by High Technology Research and Development Program of China (Grant No. 2007AA120701).

REFERENCES

1. Wu, T. K., *Frequency Selective Surface and Grid Array*, Wiley, New York, 1995.
2. Munk, B. A., *Frequency Selective Surfaces: Theory and Design*, Wiley, New York, 2000.
3. Zhang, J.-C., Y.-Z. Yin, and J.-P. Ma, "Design of narrow band-pass frequency selective surfaces for millimeter wave applications," *Progress In Electromagnetics Research,* Vol. 96, 287–298, 2009.
4. Nguyen, T. K., T. A. Ho, I. Park, and H. Han, "Full-wavelength dipole antenna on a GaAs membrane covered by a frequency selective surface for a terahertz photomixer," *Progress In Electromagnetics Research,* Vol. 131, 441–455, 2012.
5. Wu, X., Z.-B. Pei, S.-B. Qu, Z. Xu, J.-Q. Zhang, H. Ma, and X.-H. Wang, "Design and experimental Verification of band-pass Frequency Selective Surface Based on metamaterial Effective Medium Theory," *Journal of Infrared and Millimeter Waves*, Vol. 30, No. 5, 469–474, 2011.
6. Zhu, X., W. Shao, J.-L. Li, and Y.-L. Dong, "Design and optimization of low RCS patch antennas based on a genetic algorithm," *Progress In Electromagnetics Research,* Vol. 122, 327–339, 2012.
7. Jian, L., G. Xu, J. Song, H. Xue, D. Zhao, and J. Liang, "Optimum design for improving modulating-effect of coaxial magnetic gear using response surface methodology and genetic algorithm," *Progress In Electromagnetics Research,* Vol. 116, 297–312, 2011.
8. Monacelli, B., J. B. Pryor, B. A. Munk, D. Kotter, and G. D. Boreman, "Infrared frequency selective surface based on circuit-analog square loop design," *IEEE Transactions on Antennas and Propagation*, Vol. 53, No. 2, 745–752, 2005.
9. Weile, D. S. and E. Michielssen, "Genetic algorithm optimization applied to electromagnetics: A review," *IEEE Transactions on Antennas and Propagation*, Vol. 45, No. 3, 343–353, 1997.
10. Monavar, F. M. and N. Komjani, "Bandwidth enhancement of microstrip patch antenna using jerusalem cross-shaped frequency

selective surfaces by invasive weed optimization approach," *Progress In Electromagnetics Research*, Vol. 121, 103–120, 2011.

11. Biber, S., M. Bozzi, O. Gunther, L. Perregrini, and L. P. Schmidt, "Design and testing of frequency selective surfaces on thick silicon substrate operating at 600 GHz," *IEEE Microwave Conference*, Vol. 1, European, 2005.
12. Ohira M., H. Deguchi, M. Tsuji, and H. Shigesawa, "Multiband single-layer frequency selective surface designed by combination of genetic algorithm and geometry-refinement technique," *IEEE Transactions on Antennas and Propagation*, Vol. 52, No. 11, 2925–2931, 2004.
13. Monorchio, A., G. Manara, U. Serra, G. Marola, and E. Pagana, "Design of waveguide filters by using genetically optimized frequency selective surfaces," *IEEE Microwave and Wireless Components Letters*, Vol. 15, No. 6, 407–409, 2005.
14. Gingrich, M. A. and D. H. Werner, "Synthesis of low/zero index of refraction metamaterials from frequency selective surfaces using genetic algorithms," *Electronics Letters*, Vol. 41, No. 23, 1266–1267, 2005.
15. Djabery R., S. Nikmehr, and S. Hosseinzadeh, "Grating effects on sidelobe suppression in MIM plasmonic filters," *Progress In Electromagnetics Research*, Vol. 135, 271–280, 2013.
16. Brennan, P. V., A. Narayanan, and R. Benjamin, "Grating lobe control in randomised, sparsely populated MIMO radar arrays," *IET Radar, Sonar & Navigation*, Vol. 6, No. 7, 587–594, 2012.
17. Manara, G., A. Monorchio, and R. Mittra, "Frequency selective surface design based on genetic algorithm," *Electronics Letters*, Vol. 35, No. 17, 1400–1401, 1999.
18. Min, K. I., S. H. Ha, S. W. Lee, and Y. H. Moon, "Transmission loss allocation algorithm using path-integral based on transaction strategy," *IEEE Transactions on Power Systems*, Vol. 25, No. 1, 195–205, 2010.
19. Raynolds, J. E., B. A. Munk, J. B. Pryor, and R. J. Marhefka, "Ohmic loss in frequency-selective surfaces," *Journal of applied physics,* Vol. 93, No. 9, 5346–5358, 2003.
20. Su, J., X.-W. Xu, M. He, and K. Zhang, "Integral-equation analysis of frequency selective surfaces using Ewald transformation and lattice symmetry," *Progress In Electromagnetics Research*, Vol. 121, 249–269, 2011.